SPE Brazil Flow Assurance Technology Congress
Rio de Janeiro, Brazil, November 15 – 18 2022

Hydrate Plug Removal Through One-sided Depressurization in Gas-Condensate Pipelines

Rodrigo L. F. Castello Branco[1*], Claudio V. Barreto[2], Pedro Serrano[2], Adriana Teixeira[3], Leandro S. Valim[3], Angela O. Nieckele[1]
[1]Department of Mechanical Engineering, PUC-Rio, Brazil * rcastello@puc-rio.br
[2]SIMDUT, PUC-Rio, Brazil
[3]CENPES, Petrobras, Brazil

Abstract
One-sided depressurization is often employed in hydrate plug removal processes and has inherent risks associated with the high velocities achieved by the plug due to the pressure differential. In critical conditions, events such as pipeline rupturing may occur. Thus, a need for detailed numerical studies to aid in the risk reduction of such operations is paramount. The present work devises a numerical methodology to predict the dynamics of plugs in transient two-phase flow conditions, coupled with a compositional model to determine the formation of gas condensate. A complex case study is evaluated under different one-sided depressurization conditions and different plugs sizes. The contact force coefficient was neglected in all but one of the cases, so that more extreme situations can be explored. Results showed that the pressure differential led to a steep increase of the plug velocity, followed by a smooth decrease over time. The changes in the operating conditions had significant influence on the peak values of temperatures, velocities, and condensate formation, but all simulated operations were able to remove the plug from the pipeline.

Keywords
Hydrate plug; One-sided Depressurization; Phase change.

Introduction

With the advancement of deep-water oil and gas exploration, flow assurance becomes an ever-present challenge in offshore production systems, especially considering the increasing lengths of the pipeline systems and the uneven terrain upon which these structures are built. The low temperature and high-pressure environment creates a predisposition for blockage due to hydrate plugs, which impairs further production and causes substantial economic loss. To deal with the challenge of hydrate formation, two main approaches are employed in the industry: avoidance (using inhibitors, thermal insulation, and heating) and management (through the monitoring of hydrate formation, and its removal) [1].

For scenarios where hydrate plugs occur, a removal process must be carried out. A frequently used method is pipeline depressurization, which partly dissociates and dislodges the plug from the pipeline walls [2]. Although two-sided depressurization is safer, there is often limited access to the well side of the pipeline. In one-sided depressurization, both pipe extremities are closed, and pressure in one end is reduced, so that the plug will be displaced by the pressure jump across it. With the plug movement, while gas is compressed downstream, it is decompressed upstream, and the plug will stop when both pressures balance. However, it has inherent risks associated with the high acceleration and velocities achieved by the plug due to the initial pressure differential. In critical conditions, pipeline rupturing and temperatures above or below the pipeline specification limits may occur [3].

These conditions impose a significant need for detailed mathematical and numerical studies to aid in the risk reduction of such operations. Several works have devised methodologies to predict hydrate plug movement through pipelines undergoing depressurization [2-5]. From numerical simulations, one can obtain valuable information such as the peak velocity of the plug, variations of pressure and temperature along with the displacement of the plug, and stoppage conditions. During depressurization operations, depending on the hydrocarbon composition of the natural gas, a significant rate of condensation may occur, which poses an additional challenge for the numerical modeling, as a compositional model of phase equilibrium is required [6].

The present work devises a rigorous numerical methodology to predict the dynamics of hydrate plugs in transient two-phase flow conditions, coupled with a compositional model to accurately determine the formation of gas condensate.

A complex case study of a transport flowline and riser is evaluated with the novel approach under different one-sided depressurization conditions, for different plugs sizes.

Methodology

The methodology of the present work is subdivided in the governing two-phase flow equations, the plug dynamic model, the thermodynamic model, and the numerical method.

Governing Equations

In the presence of condensate, the flow becomes two-phase, with each phase identified with its volumetric fraction α_k , where the subscript k can be equal to G or L (gas or liquid). Volumetric fractions must respect the following restriction $\alpha_L + \alpha_G = 1$. Here, the mixture homogeneous model was employed. Due to the small amount of condensate, gas and condensate are uniformly distributed and flow at the same velocity u_m. The mixture enthalpy h_m and density ρ_m are

$$h_m = \frac{\alpha_L \rho_L h_L + \alpha_G \rho_G h_G}{\rho_m} \quad ; \quad \rho_m = \alpha_L \rho_L + \alpha_G \rho_G \qquad (1)$$

The conservation equations are obtained by combining the conservation equation for each phase, therefore, interfacial terms disappear. Since the pipelines are very long, a 1D approximation is employed. Let's consider a pipeline with diameter D (cross section area $A = \pi D^2/4$, perimeter $S_s = \pi D$), which can vary along the pipeline, and inclined at θ with the horizontal direction. Considering the dependence of density and enthalpy in the pressure, P, temperature T and volume fraction α, the conservation equations can be written as

$$\frac{DP}{D\,t} + \rho_m a_m^2 \left[\frac{\partial u_m}{\partial s} + \frac{u_m}{A}\frac{\partial A}{\partial s} - \beta_m \frac{DT}{Dt} + \frac{(\rho_G - \rho_L)}{\rho_m}\frac{D\alpha_G}{Dt}\right] = 0 \qquad (2)$$

$$\frac{D\,u_m}{D\,t} = -\frac{1}{\rho_m}\frac{\partial P}{\partial s} - g\,sin\,\theta - \frac{\tau_s\,S_s}{\rho_m\,A} = 0 \qquad (3)$$

$$\frac{DT}{Dt} = \frac{q_s^{"}\,S_s}{\rho_m cp_m\,A} + \frac{(\alpha_G\,\beta_G + \alpha_L \beta_L)\,T}{\rho_m cp_m}\frac{D\,P}{Dt} + \frac{P}{\rho_m cp_m}\frac{1}{A}\left(\frac{\partial A}{\partial P}\right)\frac{\partial P}{\partial t} + \frac{\tau_s\,S_s\,u_m}{\rho_m cp_m\,A} - \frac{\lambda}{cp_m}\frac{D\,\chi_G}{Dt} \qquad (4)$$

where t and s represent the time and spatial coordinate, and g is the gravitational acceleration. The material derivative is $D/Dt = \partial/\partial\,t + u_m\,\partial/\partial\,s$. The mixture properties are: isothermal sound velocity, a_m^2; thermal expansion coefficient, β_m; mixture specific heat at constant pressure cp_m; latent heat, $\lambda = h_G - h_L$; gas molar fraction $\chi_G = \alpha_G\,(\rho_G/\rho_m)(\overline{Mw}/Mw_G)$, where Mw_G and $\overline{Mw} = \sum_i z_i\,Mw_i$ are the gas and total molar weights, based on the molar composition z_i (subscript i indicates a component). The wall shear stress τ_s and heat flux from the ambient $q_s^{"}$ are

$$\tau_s = (f/4)\,\rho_m\,|u_m|\,u_m/2 \quad ; \quad q_s^{"} = U_T(T_\infty - T) \qquad (5)$$

where f is the friction factor, given by the Lockart-Martinelli correlation [7]. $U_T = 1/(h_{in}^{-1} + U_G^{-1})$ is the external overall heat transfer coefficient. h_{in} is the heat transfer coefficient between the mixture and the wall, and it can be determined with Gnienlisk correlation [8], while U_G is the global heat transfer coefficient related to the pipe wall and insulations and heat transfer coefficient to the ambient, at temperature T_∞.

Plug Dynamics

As a first approximation, hydrate melting, and gas vaporization were not considered. The plug movement is modeled by a balance force equation

$$m_p \frac{dV_p}{dt} = (P_1 - P_2)A - m_p\,g\,sen\,\theta - (F_d + C_d V_p) \qquad (6)$$

where m_p is the plug mass (constant), defined in terms of the hydrate density and porosity. $V_p = ds_p/dt$ is the plug velocity. P_1 and P_2 are the pressure values at the upwind and downwind faces of the plug. The contact force is modeled as a combination of a constant contact force F_d and constant dynamic coefficient C_d.

Initial and boundary conditions

For unilateral depressurization cases, initially there is no flow due to plug blockage, with gas in thermal equilibrium with the external environment. Both pipe extremities are closed, and pressure in one end is reduced, so that the plug will be displaced by the pressure jump across it. The initial pressure distribution corresponds to the hydrostatic pressure.

Gas Properties and Thermodynamic Model

The gas is modeled based on the equation of state of Peng-Robinson [9]

$$\rho_k = P\,Mw_k/(\,Z_k\,\Re\,T) \qquad (7)$$

where $Z_k(P,T)$ is the compressibility factor of phase k (G or L). To determine the condensate formation, a FLASH algorithm [10] is employed, equating the liquid and gas fugacities of all species i, employing the Newton's method. As a result, the mass fraction of each species in each phase is obtained, as well as both phase properties, the liquid holdup and the mixture properties. The mixture viscosity is based on the volume fraction of each phase and correlations for the gas [11] and liquid viscosities [12].

Numerical Model

The conservation equations, along with their initial and boundary conditions are solved numerically through the Finite Difference Method in a staggered and moving grid. The spatial derivatives were approximated with an Upwind scheme, and the time integration was performed with a 1st order Euler implicit schemed with a semi-implicit method. The resulting numerical system consists of a hepta-diagonal matrix, which can be solved directly.

Case Study

An 11.3 km pipeline, with 6 in internal diameter, composed by a flowline and a riser, shown in Fig. 1, is selected for the analysis. The external overall is heat transfer coefficient is U_T= 5.3 W/(m^{2}K) at the flow line and riser. The environmental temperature is 4ºC at the sea bottom and increases to 11.2ºC at

the surface. The natural gas composition is defined in Tab. 1.

A hydrate plug is positioned at $s = 2$ km from the well-head (see Fig. 1), with porosity of 5 %. An extreme condition was considered, neglecting any contact resistance ($F_d = C_d = 0$). At the well-head, the pressure is $P_{up} = 450$ bar. The operation to displace different plug lengths are considered, $L = 1m, 10m$, and $100m$. To displace the plug with unilateral depressurization, different downstream pressure were also examined (P_{dn} = 1 bar and 10 bar). An additional test was performed to evaluate the impact of plug resistance to its movement.

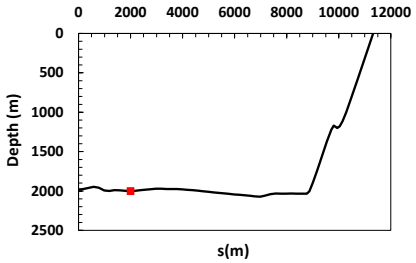

Figure 1. Case study geometry.

Table 1. Gas composition.

Component	C1	C2	C3	iC4	nC4	nC5	CO_2
Composition %	45	7	4	1	2	1	40

Results and Discussion

To analyze the solution along the pipeline at different time instants, one case was selected ($L = 10m, P_{dn} = 10\ bar, F_d = C_d = 0$). Figure 2 illustrates the time evolution of the plug, as well as its velocity as a function of its position. Pressure, velocity, temperature and holdup profiles along the pipeline for different time instants are shown in Fig. (3). Figure 4 shows the pressure × temperature pair along the duct, superimposed with the phase envelope, for different instants of time.

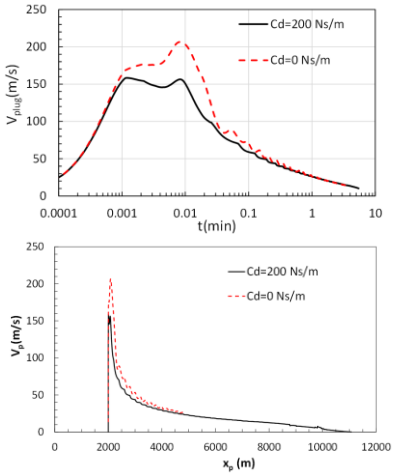

Figure 2. Time evolution of the plug velocity, plug velocity × plug position. $L = 10m, P_{dn} = 10\ bar$.

The high differential pressure in the onset of the dislodging of the plug, in the absence of a contact force resistance, leads to very high plug velocities, but for a very short time interval (Fig. 2). After this fast initial transient, the plug moves with a much lower velocity, which decays very slowly.

It can be clearly seen in Fig. 3 the depressurization upstream of the plug with an increase in pressure downstream. The high-pressure difference inducing the plug displacement leads to an increase in gas velocity. As the pipeline extremities are closed, a reflection of the flow is also observed at the end, leading to a flow reversal. The high depressurization upstream of the plug causes a decrease in temperature, while the pressure increase downstream has the opposite effect. Additionally, due to viscous dissipation, a large temperature increase can be observed near the plug position. Analyzing the holdup distribution, together with the envelope in Figure 4, it is observed that the gas at the beginning of the process is in the supercritical region. With depressurization, the gas enters the envelope, however, the lower pressures and high temperatures downstream of the plug are in the saturated gas region.

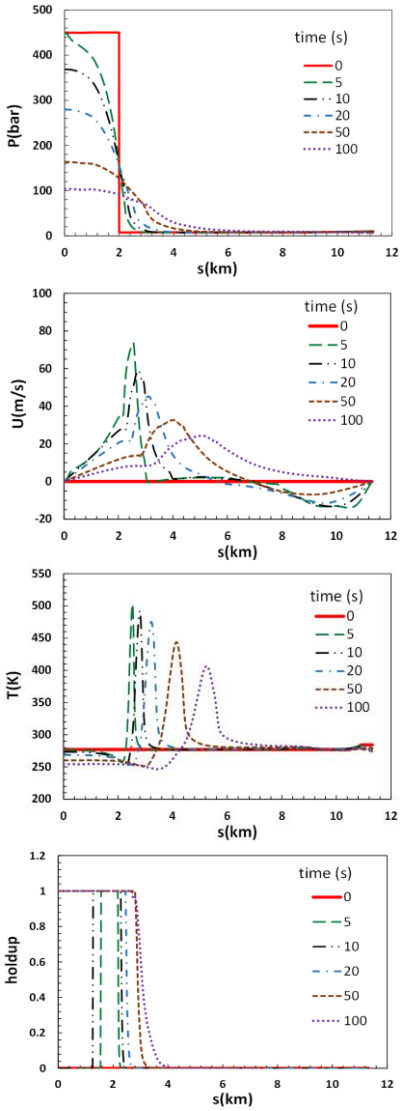

Figure 3. Spatial variation of the pressure, velocity, temperature and holdup at different times. $L = 10m, P_{dn} = 10\ bar, F_d = C_d = 0$.

Considering the same plug and operating conditions, Figure 2 also shows the plug velocity and

its position obtained in the presence of a contact resistance proportional to its velocity ($C_d = 200$ Ns/m). The plug velocity time and space evolutions are very similar, with smaller maximum plug velocity.

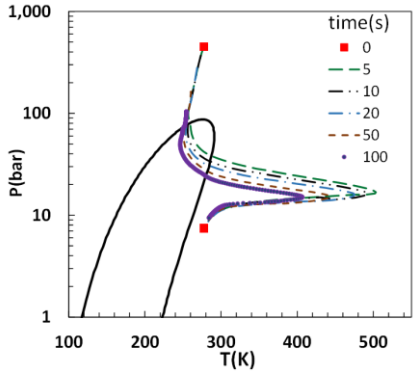

Figure 4. Pressure x temperature along the pipeline at different instants, superimposed in gas envelope,$L = 10m, P_{dn} = 10\ bar, F_d = C_d = 0$.

Examining Table 2, one can see that the reduction of the driving force leads to smaller maximum plugs velocities and temperatures, as well as in the presence of longer plugs, as expected. Note also, the reduction on the volume of condensate for these situations. In all cases examined here, the plug reaches the exit, however the longer plug ($L = 100$m) takes a very long time, since it presents difficulty to overtake the buoy region, as can be seen in Fig. 5. Due to the lower velocity obtained in the presence of a contact resistance, smaller maximum temperatures are also obtained, resulting also in a lower amount of formed condensate.

Table 2. Impact of depressurization, plug size and contact force

P_{dn} (bar)	L (m)	$\forall_{cond}$ (Sd m³)	$V_{p_{max}}$ (m/s)	$T_{p_{max}}$ (°C)	C_d (Ns/m)
1	1	21.8	473	625	0
	10	10.1	463	234	0
10	1	23.5	273	604	0
	10	14.3	207	220	0
	100	9.26	149	238	0
	10	12.5	158	128	200

Conclusions

Risk reduction in one-sided depressurization operations is paramount for the adequate flow assurance management. The present model can be very helpful in planning this type of operation.

Due to the uncertainty in the contact force coefficient, it can be neglected, so that extreme situations can be explored. Results showed that the pressure differential resulted in a steep increase of the plug velocity, but for a very short period of time. For all cases tested here, the operation was successful, as the plug reached the pipe outlet, but for others operating conditions, this might not be true. In future work, flow pattern dependence must be included to better represent the two-phase phenomena. The present type of analysis is a powerful tool to plan this kind of operation, in order to be safe and successful.

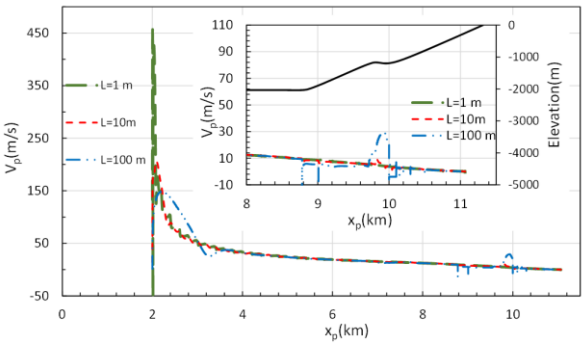

Figure 5. Spatial variation of the plug velocity, compared with the elevation of the pipeline in the buoy region. $P_{dn} = 10\ bar, F_d = C_d = 0$.

Acknowledgments

The authors wish to thank Petrobras, CNPq and CAPES for supporting the development of this work.

Responsibility Notice

The authors are the only responsible for the paper content.

References

[1] De Almeida, V.; Serris, E.; Cameirão, A.; Herri, J.; Abadie, E.; Glénat, P. J. Natural Gas Science and Engineering. 97, 104338, 2022

[2] Xiao, J. J.; Shoup, G.; Hatton, G.; Kruka, V. Offshore Technology Conference, 8728, pp.161, Houston, Texas, 1998

[3] Golçalves, M.; Camargo, R.; Nieckele, A. O.; Furaco, R.; Barreto, C. V.; Pires, L. F. G. ASME 2012 31st Int. Conf. Ocean, Offshore and Arctic Eng., OMAE2012-83969, RJ, Brazil, 2012

[4] Camargo, R.; Gonçalves, M.; Barreto, C.; Faraco, R.; Nieckele, A.O. 7th International Conference on Gas Hydrates, Edinburgh, Scotland, United Kingdom, 2011

[5] Yang, M.; Ma, Z.; Gao, Y.; Jiang, L. Chinese J. Chem. Eng. 27, 2089-2098, 2019.

[6] Branco, T.; Nieckele, A. O.; Pires, L. F. G.; Veloso, C.; Tavares, F. W., Segtovich, I. S. V.; do Carmo, R. P.; da Silva, V. M.; Fonseca Jr.,R.; Valim, L. 5-6th Thermal and Fluids Engineering Conference (TFEC), Virtual, 2021

[7] Lockhart, R. W., Martinelli, R. C., Chem. Eng. Prog., 45(1), 39-48, 1949

[8] Incropera, F.P., DeWitt, D.P., Bergman, T.L. Lvine, A.S., Fundamentals of Heat and Mass Transfer, 2008

[9] Nichita, D. V.; Leibovici, C. F.; Improved solution windows for the resolution of the Rachford-Rice equation. Fluid Phase Equilibria, 452, 69–73, 2017.

[10] Pratt, R. M., Chem. Eng. Education, 2001

[11] Lee, A. L., Gonzalez, M.H., Eakin, B. E., J. Petroleum Technology, 18, 997–1000, 1966.

[12] Lee, A. L., Gonzalez, M.H., Eakin, B. E., *J. Petroleum Technology,* 18, 997–1000, 1966.

[13] Lohrenz, J.; Bray, B. G.; Clark, C. R., J Petr Technol - SPE-915-PA, 1171-1176, 1964.